Neutron Diffraction Study of Quenched $Li_{0.3}La_{0.567}TiO_3$ Lithium Ion Conducting Perovskite

Marco Sommariva and Michele Catti*

Dipartimento di Scienza dei Materiali, Università di Milano Bicocca, via Cozzi 53, 20125 Milano, Italy

Received January 17, 2006. Revised Manuscript Received March 7, 2006

The Li^+ ion conductor $Li_{0.3}La_{0.567}TiO_3$ was synthesized as a metastable phase quenched in liquid N_2 from 1300 °C, and it was studied by time-of-flight powder neutron diffraction at high-resolution (HRPD instrument, ISIS Facility, U.K.). At room temperature a tetragonal perovskite superstructure was found, with a $\sqrt{2}a_p \times \sqrt{2}a_p \times 2a_p$ unit cell ($a = 5.48027(1)$, $c = 7.75591(2)$ Å, and $Z = 4$), *I*4/*mcm* space group, and $a^0a^0c^-$ tilt system of the TiO_6 octahedra. Superlattice *hkl* reflections with odd *l* were systematically weaker and broader. By Fourier difference maps, the Li atom was located in a disordered position inside the La vacancy hollow, close to the bottleneck site at the center of the Ti_4O_4 square window. The Rietveld refinement converged to $R_p = 6.56\%$, R_{Bragg}(even *l*) = 3.26%, and R_{Bragg}(odd *l*) = 11.6%. A two-dimensional pathway of Li^+ ion mobility inside the structure, based on the coupled ordering of lithium and lanthanum, is proposed. At about 600 °C the unit cell transforms into $a_p \times a_p \times a_p$, with a disappearance of superlattice reflections. A tetragonal pseudo-cubic *P*4/*mmm* structure ($a = 3.89644(1)$, $c = 3.89748(2)$ Å, and $Z = 1$) was found ($T = 650$ °C) and Rietveld refined to $R_p = 6.10\%$ and $R_B = 4.86\%$. Lithium was located on the layer of Ti atoms rather than on that of La as in the room-temperature structure.

Introduction

The perovskite structure, though very simple in its basic configuration, is well-known to be associated with an amazing variety of chemical compositions, physical properties, and crystallographic variations. In particular, the physicochemical behavior of perovskites is strongly affected by phase transitions, which usually occur with great ease within the symmetry group−subgroup constraint. It often happens that the interesting property of the perovskite material is present or strongly enhanced only in one of its phases, which are related by small crystallographic distortions to the basic cubic structure. This is likely to occur also for the family of lithium perovskites, which display a high alkali ion mobility and then are of great importance as cathode materials or solid electrolytes in lithium batteries and other electrochemical devices.[1,2]

We are interested here in the $Li_xLa_{2/3-x/3}\square_{1/3-2x/3}TiO_3$ (LLTO) system, which is one of those showing the highest lithium ion electrical conductivity at room temperature (RT; about 10^{-3} S cm^{-1} for $x = 0.3$).[3,4] In Li-free $La_{2/3}\square_{1/3}TiO_3$, lanthanum occupies on the average 2/3 of the A sites of the ABO_3 perovskite structure, whereas 1/3 are vacant.[5] Lithium insertion occurs by partly replacing La atoms and partly occupying the hollows around the empty A sites; when $x = 0.5$, all the A sites are saturated by either La or Li. Clearly, the extended disordered distribution of lithium atoms and vacancies is responsible for the high ionic mobility. However, although several structural studies of this system at a number of Li compositions have been performed, only in a few cases lithium could be reliably located by the choice technique of neutron diffraction.[6−9] This task is particularly difficult in case of small Li content (say, $x < 0.25$), where a problem of scattering sensitivity arises. Further, many crystallographic variations on the theme of the basic perovskite structure were detected or hinted at in previous work on the LLTO system, suggesting that the subject is far from being exhausted and that it is crucial to clarify the lithium distribution and then the structural basis of ionic mobility.

Many authors pointed out that conventional X-ray powder diffraction (XRPD) is not able to detect deviations from the standard perovskite cubic cell ($a_p \approx 3.87$ Å), whereas by electron diffraction, transmission electron microscopy (TEM), and neutron diffraction several types of symmetry lowering, with different superlattices with respect to the basic perovskite cell, were found. The lithium content (*x* value) and the cooling rate in the sample synthesis play a crucial role in this respect. In particular, for slowly cooled samples with low Li content ($0.12 \leq x \leq 0.20$) an orthorhombic *Cmmm* or *Cm2m* phase with cells of type $2a_p \times 2a_p \times 2a_p$ was found,[8−13] but on quenching the $x = 0.18$ sample in liquid

* Corresponding author. E-mail: catti@mater.unimib.it.

(1) Belous, A. G.; Novitskaya, G. N.; Polyanetskaya, S. V.; Gornikov, Y. I. *Russ. J. Inorg. Chem.* **1987**, *32*, 156.
(2) Stramare, S.; Thangadurai, V.; Weppner, W. *Chem. Mater.* **2003**, *15*, 3974.
(3) Inaguma, Y.; Liquan, C.; Itoh, M.; Nakamura, T.; Uchida, T.; Ikuta, H.; Wakihara, M. *Solid State Commun.* **1993**, *86*, 689.
(4) Kawai, H.; Kuwano, J. *J. Electrochem. Soc.* **1994**, *141*, L78.
(5) Kim, I.-S.; Nakamura, T.; Inaguma, Y.; Itoh, M. *J. Solid State Chem.* **1994**, *113*, 281.
(6) Ruiz, A. I.; López, M. L.; Veiga, M. L.; Pico, C. *J. Solid State Chem.* **1999**, *148*, 329.
(7) Alonso, J. A.; Sanz, J.; Santamaria, J.; León, C.; Varez, A.; Fernández-Diaz, M. T. *Angew. Chem., Int. Ed.* **2000**, *39*, 619.
(8) Inaguma, Y.; Katsumata, T.; Itoh, M.; Morii, Y. *J. Solid State Chem.* **2002**, *166*, 67.
(9) Varez, A.; Inaguma, Y.; Fernández-Diaz, M. T.; Alonso, J. A.; Sanz, J. *Chem. Mater.* **2003**, *15*, 4637.

10.1021/cm060120r CCC: $33.50
Published on Web 04/04/2006

N_2 the rhombohedral $R\bar{3}c$ symmetry appeared instead.[9,14] With the Li-richest composition ($x = 0.5$), again different results are reported for slowly cooled and for quenched samples: in the former case, a $P4mm$ symmetry with a $\sqrt{2}a_p \times \sqrt{2}a_p \times 2a_p$ unit cell was observed by TEM,[15] whereas in the second one the $R\bar{3}c$ structure is indicated.[7,12]

Our interest is focused upon the intermediate $x = 0.3$ composition, to which comparatively less attention was paid, despite its very good ionic conductivity performance. To our knowledge, the only reported neutron diffraction investigation ($x = 0.31$, nonquenched sample)[6] proposed a $P4/mmm$ structure with a $a_p \times a_p \times 2a_p$ unit cell, similar to that already suggested for a wider composition range on the basis of TEM results.[16] However, in this structure lithium was assumed to lie exactly at the place of lanthanum, giving rise to Li−O bond distances of 2.7 Å, which are unrealistically long. Later a combined TEM−X-ray synchrotron radiation study of the $x = 0.35$ composition (sample quenched to RT) appeared,[17] where the unit cell of type $\sqrt{2}a_p \times \sqrt{2}a_p \times 2a_p$ was proposed, with a Rietveld refined (of course, without lithium because of its low X-ray scattering factor) orthorhombic $Pmma$ structure.

We have thus undergone a new investigation of the $Li_{0.3}La_{0.567}TiO_3$ material by high-resolution time-of-flight neutron diffraction techniques, with a particular emphasis on studying the structural effects of the quenching step in the preparation of the sample.

Experimental Section

Synthesis and X-ray, Thermal, and Chemical Analyses. The $Li_{0.3}La_{0.567}TiO_3$ compound was synthesized by solid-state reaction.[9,18] A preliminary drying and decarbonating treatment was carried out for some hours at different temperatures on the Li_2CO_3 (110 °C), TiO_2 (600 °C), and La_2O_3 (850 °C) reagents, which were then mixed in stoichiometric ratios, ground with acetone in a mortar, and heated at 900 °C for 5 h to decompose the carbonate. After further grinding, the powder was pelletized and finally heated at 1300 °C for 6 h in a platinum crucible. To prevent lithium evaporation, the pellet was covered with a powder of the same composition. The pellet sample was quenched from 1300 °C in liquid nitrogen. By XRPD (Bruker D8 Advance equipment, Cu Kα radiation, step time 8 s), a pure single phase was detected with sharp and intense Bragg peaks, which could be indexed and accounted for on the basis of a standard cubic perovskite structure (space group $Pm\bar{3}m$, refined cell edge $a_p = 3.876(1)$ Å). No extra peaks appeared in the diffractogram.

A chemical analysis was performed to determine the lithium content. The sample was dissolved into a 3:2:1 volume mixture of concentrated acid solutions (HNO_3 65%, HCl 37%, HF 48%) and heated at 200 °C for 30 h. On leaching an insoluble residue remained and was filtered, and the solution was analyzed for lithium by flame emission spectrophotometry, obtaining a result of 0.26 Li atoms per formula unit (pfu). XRPD on the solid residue showed the presence of TiO_2 and of unidentified phases, surely lanthanum compounds. It cannot be excluded that a small fraction of Li remained chemically bonded in the insoluble powder. Therefore, we conclude that the possible lithium loss with respect to nominal composition in the synthesized compound has an upper bound of 13%; for simplicity, the nominal content of 0.30 Li atoms pfu will be assumed henceforth.

The thermal behavior of the synthesized compound was studied by a differential thermal analysis (DTA) experiment in the 25−1000 °C temperature range (Perkin-Elmer equipment, 20 and 10 °C min^{-1}, heating and cooling runs). No peaks or anomalies could be detected in the explored thermal interval.

Neutron Scattering Measurements. Neutron diffraction data were collected on the time-of-flight high-resolution powder diffractometer (HRPD) at the ISIS pulsed spallation source, Rutherford Appleton Laboratory (Chilton, U.K.). A powder specimen of about 2 cm^3, put in a vanadium can under vacuum, was employed. By use of the backscattering counter bank at $2\theta = 168.3°$, a full intensity profile was collected in the d_{hkl} range 0.68−2.5 Å with high resolution of $\Delta d/d \approx 4 \times 10^{-4}$ at 25 °C (8 h). Patterns recorded at lower resolution on the $2\theta = 90°$ (0.94 to 3.2 Å) and $2\theta = 30°$ (2.6 to 8.9 Å) counter banks were also taken into account for indexing and unit cell determination purposes. Then the can was surrounded by a resistance furnace, and data were collected in short runs at several temperatures, detecting a phase transition at about 600 °C by a qualitative change of the diffraction pattern. A long run (10 h) was then carried out at 650 °C.

Preliminary data reductions were performed, including merging of outputs from single counters in the bank and correction for detector efficiency as a function of neutron wavelength. The Rietveld refinements of the crystal structures of $Li_{0.3}La_{0.567}TiO_3$ at both temperature values (high-resolution patterns) were carried out by the FULLPROF computer package.[19] A linear combination of six polynomials was used to model the intensity background, and the peak shape was represented by a convolution of a pseudo-Voigt function (linear combination of Gaussian and Lorentzian components, with σ and γ half-widths, respectively; sample contribution) with two back-to-back exponentials (instrumental and moderator contributions).[20] The σ and γ parameters were assumed to depend on d_{hkl} according to the following formulas: $\sigma = (\sigma_2 d_{hkl}^4 + \sigma_1 d_{hkl}^2 + \sigma_0)^{1/2}$ and $\gamma = \gamma_2 d_{hkl}^2 + \gamma_1 d_{hkl} + \gamma_0$. The mixing coefficient and the full width of the pseudo-Voigt function depend on σ and γ according to equations given in the literature.[21]

Results

RT Structure. The neutron diffraction Bragg peaks of the 25 °C pattern were indexed by the DICVOL program,[22] which unambiguously indicated a body-centered tetragonal unit cell of type $\sqrt{2}a_p \times \sqrt{2}a_p \times 2a_p$. This was fully

(10) Sanz, J.; Alonso, J. A.; Varez, A.; Fernández-Diaz, M. T. *J. Chem. Soc., Dalton Trans.* **2002**, 1406.
(11) Sanz, J.; Varez, A.; Alonso, J. A.; Fernández-Diaz, M. T. *J. Solid State Chem.* **2004**, *177*, 1157.
(12) Varez, A.; Fernández-Diaz, M. T.; Alonso, J. A.; Sanz, J. *Chem. Mater.* **2005**, *17*, 2404.
(13) Yashima, M.; Itoh, M.; Inaguma, Y.; Morii, Y. *J. Am. Chem. Soc.* **2005**, *127*, 3491.
(14) Rivera, A.; Sanz, J. *Phys. Rev. B* **2004**, *70*, 094301.
(15) Varez, A.; Garcia-Alvarado, F.; Morán, E.; Alario-Franco, M. A. *J. Solid State Chem.* **1995**, *118*, 78.
(16) Fourquet, J. L.; Duroy, H.; Crosnier-Lopez, M. P. *J. Solid State Chem.* **1996**, *127*, 283.
(17) Garcia-Martin, S.; Alario-Franco, M. A.; Ehrenberg, H.; Rodriguez-Carvajal, J.; Amador, U. *J. Am. Chem. Soc.* **2004**, *126*, 3587.
(18) Varez, A.; Ibarra, J.; Rivera, A.; Leon, C.; Santamaria, J.; Laguna, M. A.; Sanjuan, M. L.; Sanz, J. *Chem. Mater.* **2003**, *15*, 225.
(19) Rodriguez-Carvajal, J. FULLPROF: a program for Rietveld Refinement and Pattern Matching Analysis. http://www-llb.cea.fr/fullweb/powder.htm (accessed Sept 2005).
(20) Von Dreele, R. B.; Jorgensen, J. D.; Windsor, C. G. *J. Appl. Crystallogr.* **1982**, *15*, 581.
(21) Thompson, P.; Cox, D. E.; Hastings, J. B. *J. Appl. Crystallogr.* **1987**, *20*, 79.
(22) Boultif, A.; Louer, D. *J. Appl. Crystallogr.* **1991**, *24*, 987.

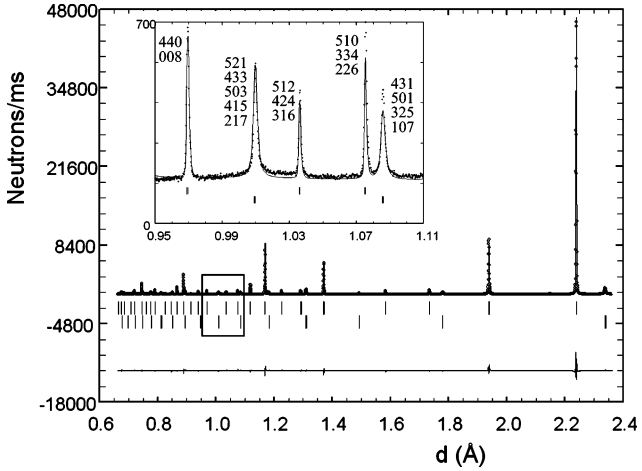

Figure 1. Time-of-flight neutron diffraction profile at RT of quenched $Li_{0.3}La_{0.567}TiO_3$. Upper peak marks denote main *hkl* reflections (*l* even) of the tetragonal *I* lattice ($\sim\sqrt{2}a_p \times \sqrt{2}a_p \times 2a_p$); lower marks correspond to superlattice reflections (*l* odd). The magnified inset shows a detailed region of the pattern with *hkl* indexes of overlapping reflections.

Table 1. Wyckoff Sites, Occupancies, Atomic Fractional Coordinates, and Displacement Factors (Å²) for the *I*4/*mcm* Structure of Quenched $Li_{0.3}La_{0.567}TiO_3$ at $T = 25$ °C (a = 5.48027(1), c = 7.75591(2) Å, and $Z = 4$)[a]

	site	occupancy	*x*	*y*	*z*	*B*
La	4b	0.567	1/2	0	1/4	0.38(2)
Ti	4c	1	0	0	0	0.74(3)
O1	8h	1	0.2759(2)	0.2241(2)	0	0.83(2)
O2	4a	1	0	0	1/4	1.95(7)
Li	16l	0.075	0.668(4)	0.168(4)	0.226(5)	2.4(8)

La−O1	2.603 × 4	Ti−O1	1.948 × 4	Li−O1	1.94(4), 2.17(4)
La−O2	2.740 × 4	Ti−O2	1.939 × 2	Li−O2	2.05(2) × 2

$R_p = 6.56\%$, $R_w = 8.80\%$, $R_B(1) = 3.26\%$, $R_B(2) = 11.6\%$

[a] The estimated standard deviations (esd's) of the refined parameters are in parentheses. Bond distances (Å) are given, with esd's, when larger than 0.001 Å. The Rietveld refinement agreement factors include those related to main (1) and superlattice (2) Bragg peaks.

confirmed by also considering the higher d_{hkl} ranges from the patterns collected at $2\theta = 90°$ and 30°. Further, two sets of *hkl* reflections could be clearly distinguished on intensity and peak-width ground: strong (narrower) and weak (broader) peaks with even and odd *l*, respectively (Figure 1). By removing the second set of reflections, the unit cell would become $a_p \times a_p \times a_p$. The crystal structure was determined by trial-and-error within the tetragonal *I*-type space groups which are subgroups of the parent $Pm\bar{3}m$ perovskite structure. In particular, the large amount of literature on the subject was taken into account, and use was also made of the Bilbao Crystallographic Server for the study of group−subgroups relationships.[23] A satisfactory structural model for Rietveld refinement was obtained only within the *I*4/*mcm* (No. 140) symmetry, with the La, Ti, and O atoms on the Wyckoff sites shown in Table 1. The chosen space group is a subgroup of index 6 of the basic cubic perovskite $Pm\bar{3}m$ (No. 221) symmetry ($a_p \times a_p \times a_p$ unit cell), from which it can be derived by a *t*3 (*translationen-gleich* (*translation-invariant*) of index 3) symmetry reduction to *P*4/*mmm* (No. 123, $a_p \times a_p \times a_p$), followed by a *k*2 (*klassen-gleich* (*class-invariant*) of index 2) further reduction to *I*4/*mcm* ($\sqrt{2}a_p \times \sqrt{2}a_p \times 2a_p$ unit cell). No body-centered tetragonal subgroups of index lower than 6 are possible, with the given unit cell relationships. The *I*4/*mcm* perovskite-derived structure is

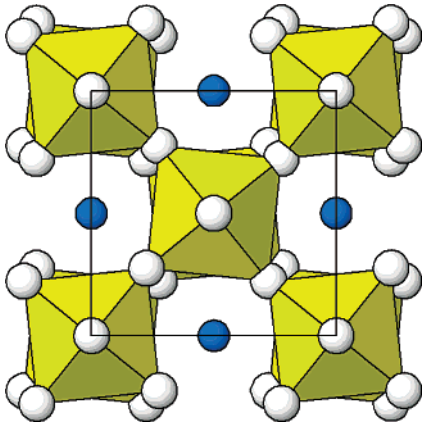

Figure 2. Projection onto the (001) plane of the *I*4/*mcm* perovskite structure of quenched $Li_{0.3}La_{0.567}TiO_3$. Dark and pale spheres represent La and O atoms, respectively, and TiO_6 coordination octahedra are emphasized. Li atoms are not shown here for simplicity.

named in the literature after that of the high-temperature (HT) phase (860−1170 °C stability range) of $SrZrO_3$,[24,25] and it corresponds to the tilt system $a^0a^0c^-$ of the coordination octahedra, according to Glazer's notation.[26] A sketch is shown in Figure 2, where the anti-phase tilting of octahedra around the *z* axis appears clearly.

Upon Rietveld refining the *I*4/*mcm* crystal structure of $Li_{0.3}La_{0.567}TiO_3$ (with no Li atoms included), problems arose to account for the peak widths of both sets of *hkl* reflections (even and odd *l* values) by use of the same peak profile function. Indeed, the systematically broader character of superlattice reflections (Figure 1) should be related to microdomain features which would require electron diffraction and TEM techniques to be fully clarified, as was done in previous studies.[16,17] A full account of sophisticated analyses of microstructural effects on the shape of XRPD peaks can also be therein found.[17] We chose a straightforward approach, allowed by the capabilities of the FULLPROF code, by introducing two distinct pseudo-Voigt functions for the two sets of reflections, with independent half-width parameters included in the refinement. This corresponds to formally refine two distinct phases with the same structural parameters but different peak-profile functions.[16] In the odd-*l* case (superlattice reflections), the peak shape was best-fitted by a pure Lorentzian function, whose half-width γ_1 parameter was in the end fixed at the value of 109, to avoid instability of the least-squares refinement. The σ_2, σ_1, and γ_1 parameters of the main reflection set (even *l*) were refined to values of 11, 228, and 16, respectively; all other profile parameters were vanishing.

The observed anisotropic broadening of the odd-*l* superlattice peaks should be surely related to a limited domain size for the coherence of the anti-phase octahedral tilts within each crystalline grain. However, whether the tilting is the primary effect of coherence loss or it is coupled to a different feature (such as, for example, lithium atom distribution)

(23) Kroumova, E.; Aroyo, M. I.; Perez Mato, J. M.; Kirov, A.; Capillas, C.; Ivantchev, S.; Wondratschek, H. *Phase Transitions* **2003**, *76*, 155.
(24) Bock, O.; Müller, U. *Acta Crystallogr., Sect. B* **2002**, *58*, 594.
(25) Ahtee, M.; Glazer, A. M.; Hewat, A. W. *Acta Crystallogr., Sect. B* **1978**, *34*, 752.
(26) Glazer, A. M. *Acta Crystallogr., Sect. B* **1972**, *28*, 3384.

driving primarily the phenomenon remains an open question at this stage of the investigation.

A Fourier difference map was then calculated and negative peaks were therein searched for, to locate Li atoms. Two evident peaks were found, n.1 with coordinates 0.609, 0.109, 0.25 and n.2 with coordinates 0.5, 0, 0.179, which showed reasonable crystal-chemical environments for possible lithium atoms. Then a single Li atom was introduced in the refinement, with either n.1 or n.2 initial coordinates, and with an occupation factor fixed at the ideal composition. In both cases the refinement converged; for the coordinates of Li n.1, see Table 1, whereas for Li n.2 the values of 0.5, 0, 0.140(3) were obtained. However, when we tried to refine two Li atoms together, with the sum of their occupation factors constrained again at ideal composition, the fractional occupation of Li n.2 drifted to a vanishing value; therefore, only Li n.1 was retained. All final refined parameters are reported in Table 1, together with the agreement factors and with the relevant interatomic distances. A significant improvement was obtained with respect to the refinement without Li atoms ($R_B(1) = 4.4\%$ and $R_B(2) = 12.0\%$).

At this point, we decided to consider also subgroups of the *I*4/*mcm* space group, with the same $\sqrt{2}a_p \times \sqrt{2}a_p \times 2a_p$ unit cell, as possible candidate symmetries for the structure of the room-temperature phase of $Li_{0.3}La_{0.567}TiO_3$. All possible cases (including orthorhombic ones) could be discarded, because they were either equivalent to the *I*4/*mcm* structure or giving much worse refinement results, with the exception of the tetragonal $I\bar{4}2m$ (No. 121) space group. In this case a reasonable structure could be refined, which is quite similar to the *I*4/*mcm* one, except for the fact that two independent La sites are present and that a very small octahedral tilt around the *x* and *y* axes is observed, in addition to that around *z* ($a^+a^+c^-$ octahedral tilt system). The Li atoms were located and refined in the same positions as in the previous case but with a halved site multiplicity. However, the final agreement indexes ($R_p = 6.81\%$, $R_w = 8.98\%$, $R_B(1) = 3.45\%$, and $R_B(2) = 11.5\%$) are higher than in the *I*4/*mcm* case, although the symmetry is lower and the number of refined parameters is larger. For this reason, the *I*4/*mcm* structure solution is considered by us to be preferable and is assumed as the correct one.

HT Structure. The neutron powder pattern collected at 650 °C is shown in Figure 3. By comparison with the corresponding room-temperature profile (Figure 1), it is clear that the set of superlattice reflections with odd *l* has disappeared, whereas all other Bragg peaks are still present. This corresponds to the basic $a_p \times a_p \times a_p$ perovskite unit cell, which can be indexed as cubic on the basis of the *d* values of the Bragg peak maxima ($a_p = 3.89680(1)$ Å). As first structure model of the HT phase of $Li_{0.3}La_{0.567}TiO_3$, then, we refined the cubic $Pm\bar{3}m$ perovskite structure ($R_p = 6.34\%$, $R_w = 8.28\%$, $R_B = 5.71\%$). In particular, the Li atom could be located on Fourier difference maps at $z = 1/2$ as Ti and refined ($x = y = 0.085(8)$), except for the displacement parameter *B* which had to be kept fixed. However, two Li−O distances out of four were very short (1.65 Å).

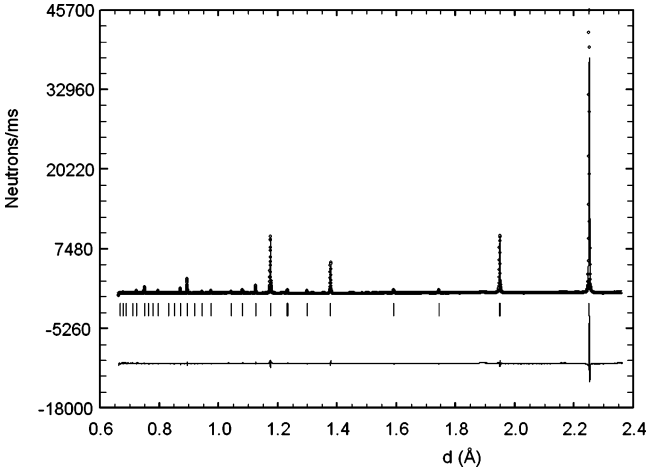

Figure 3. Time-of-flight neutron diffraction profile of $Li_{0.3}La_{0.567}TiO_3$ at 650 °C. Superlattice reflections of Figure 1 have disappeared, giving rise to a tetragonal *P* lattice with smaller unit cell ($\sim a_p \times a_p \times a_p$).

Table 2. Wyckoff Sites, Occupancies, Atomic Fractional Coordinates, and Displacement Factors (Å²) for the *P*4/*mmm* Structure of Quenched $Li_{0.3}La_{0.567}TiO_3$ at $T = 650$ °C ($a = 3.89644(1)$, $c = 3.89748(2)$ Å, and $Z = 1$)[a]

	site	occupancy	*x*	*y*	*z*	*B*
La	1a	0.567	0	0	0	0.89(4)
Ti	1d	1	1/2	1/2	1/2	1.34(6)
O1	4m	0.5	0	0.5587(10)	1/2	0.98(7)
O2	1c	1	1/2	1/2	0	2.0(1)
Li	4k	0.075	0.111(9)	0.111(9)	1/2	2.0

La−O1	2.599(3) × 8	Ti−O1	1.962(5) × 4	Li−O1	1.80(4) × 2
La−O2	2.755 × 4	Ti−O2	1.949 × 2		2.20(4) × 2

$R_p = 6.10\%$, $R_w = 7.64\%$, $R_B = 4.86\%$

[a] The estimated standard deviations (esd's) of the refined parameters are in parentheses. The Rietveld agreement factors and the bond distances (Å) are also given, with esd's, when larger than 0.001 Å.

We then looked for a more satisfactory structure model, to be represented by a space group which had to be a subgroup of $Pm\bar{3}m$ and a supergroup of *I*4/*mcm* at the same time, to keep the group/subgroup relation with the low-temperature phase. The only possible solution was *P*4/*mmm* with a slight tetragonally distorted $a_p \times a_p \times a_p$ unit cell (i.e., $a = b \neq c$). According to the discussion in the above section on the room-temperature phase, this is a *t3* subgroup of $Pm\bar{3}m$ and has *I*4/*mcm* ($\sqrt{2}a_p \times \sqrt{2}a_p \times 2a_p$) as a *k2* subgroup of its own. In a structural model of perovskite based on this space group, two independent positions (O1 and O2) arise for oxygen atoms, instead of one as in the cubic case. However, by putting O1 in the 2e position (0, 1/2, 1/2) the same previous arrangement was observed. To improve the *R* factors significantly, the O1 atom had to be given more freedom in the 4*m* site (0, *y*, 1/2), in a disordered configuration with half-occupancy.

By Rietveld refinement of the above presented *P*4/*mmm* structure, the results reported in Table 2 were obtained. A small but significant tetragonal distortion of the unit cell is observed. The agreement factors are all significantly lower than those of the $Pm\bar{3}m$ refinement, and the refined lithium coordinates now are consistent with quite reasonable Li−O distances. Therefore, the *P*4/*mmm* structural model is considered to be the correct one for the HT phase of $Li_{0.3}La_{0.567}TiO_3$. Owing to the disorder of the O1 atom, the $a^0a^0c^-$ octahedral tilting is locally preserved in this model,

although the average structural configuration requires that odd-*l* superlattice reflections vanish.

Discussion

Structural Features and Phase Transformation. The structural study of the RT phase of $Li_{0.3}La_{0.567}TiO_3$ (liquid-N_2 quenched sample) has shown unambiguously an *I*-type tetragonal $\sqrt{2}a_p \times \sqrt{2}a_p \times 2a_p$ lattice, which is the first one ever observed in the whole $Li_xLa_{2/3-x/3}\square_{1/3-2x/3}TiO_3$ system, to our knowledge. The same kind of unit cell had been previously observed for samples with $x = 0.35$ and $x = 0.5$ but associated with orthorhombic and tetragonal *P*-type lattices, respectively.[15,17] In particular, in the case of the composition closest to the present one ($x = 0.31$, non-quenched sample synthesized at 975 °C) the *P* tetragonal $a_p \times a_p \times 2a_p$ cell had been proposed,[6] with no octahedral tilting according to the $a^0a^0c^0$ scheme. Our result confirms that subtle distortions of the basic perovskite structure span a variety of possibilities in the LLTO system, also related to the maximum temperature and to the cooling rate in the synthesis process, and that their detection requires a careful use of appropriate experimental techniques. It should be also observed that in the cited study[6] the lithium position was assumed to be the same as that of lanthanum, thus attaining Li−O distances not shorter than 2.67 Å, which appear to be unrealistically long on crystal-chemical grounds. By comparison with the structural configurations of other members of the $Li_xLa_{2/3-x/3}\square_{1/3-2x/3}TiO_3$ family, we observe that the $a^0a^0c^-$ anti-phase tilting around a single axis found in the present structure is similar to the $a^0b^-c^0$ scheme of the *Cmmm* structure[8,13] of the member with $x = 0.18$, with a larger cell $2a_p \times 2a_p \times 2a_p$.

The phase transition observed around 600 °C has clearly a second-order thermodynamic character, according to DTA results, and is consistent with the group/subgroup relation between the symmetries of the two phases. The interesting feature of the HT *P*4/*mmm* structure is disorder of the O1 atom over two positions so that the $a^0a^0c^-$ tilting of Ti octahedra around the *z* axis can be locally preserved from the room-temperature structure, despite the increase of symmetry. This is at variance with the phase transitions observed in other members of the family, where the tilting disappears in the HT phase: compare the *Cmmm* ($2a_p \times 2a_p \times 2a_p$) → *P*4/*mmm* ($a_p \times a_p \times 2a_p$) and $R\bar{3}c \rightarrow Pm\bar{3}m$ transitions of the terms with $x = 0.2$ (600 °C) and 0.5 (800 °C), respectively.[11,12]

The present results show that the detailed structural features of LLTO samples depend crucially on their thermal history. In this respect, it is useful to consider previous kinetic studies performed on $Li_{0.33}La_{0.557}TiO_3$ by conventional XRPD in a range of temperatures.[27,28] The structure was therein found to display a single La site (cubic $a_p \times a_p \times a_p$) at $T > 1200$ °C and two independent La sites with different partial occupancies (tetragonal $a_p \times a_p \times 2a_p$) at lower temperature.

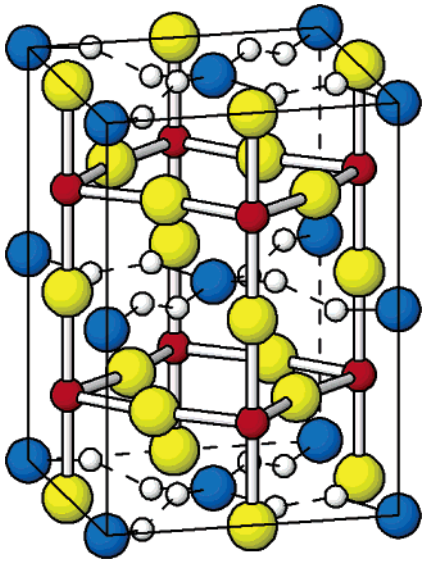

Figure 4. Unit cell content of the *I*4/*mcm* structure of quenched $Li_{0.3}La_{0.567}TiO_3$. The origin has been shifted by 1/2, 0, 1/4 with respect to the standard origin on the inversion center (cf. Figure 3 and Table 1). The lithium atoms are shown as small pale spheres. Dark and pale balls denote La and O atoms, respectively. Full and dashed lines connect Li−La and Li−Li pairs, respectively, which are not compatible in the local structure because of too short distances.

In tetragonal samples quenched from increasing temperatures and after different annealing times, a progressive disordering of La was detected by monitoring the ratio of critical Bragg peak intensities. No octahedral tilting is observed in either structure, as this requires a larger cell than $a_p \times a_p$ in the (001) plane.

In our opinion, superlattice reflections leading to the $\sqrt{2}a_p \times \sqrt{2}a_p$ lattice unit in the (001) plane and to the related $a^0a^0c^-$ octahedral tilting as in our RT structure were missed by the X-ray probe which is hardly sensitive to O atom shifts. The superstructure peaks of the neutron diffraction pattern of our quenched sample (*I* tetragonal $\sqrt{2}a_p \times \sqrt{2}a_p \times 2a_p$ cell) are only due to octahedral tilting and not to a split of the single La site into two independent ones along the *c* axis, as in *P* tetragonal $a_p \times a_p \times 2a_p$ or $\sqrt{2}a_p \times \sqrt{2}a_p \times 2a_p$ lattices. Thus, the quoted results[27,28] on convergent disordering of the La sites are consistent with the *I*4/*mcm* structure of our sample, which shows a single partially occupied La site because the quenching occurred at $T > 1200$ °C. We believe that the original stable structure at 1300 °C was probably cubic $a_p \times a_p \times a_p$ and that an incomplete quenching process has produced a metastable phase preserving the single La site, but introducing the octahedral tilting which lowers the symmetry to *I*4/*mcm*. On heating the sample in a thermal range below the quenching temperature of 1300 °C it is likely that other metastable structural states are still achieved, and so it not surprising that the transformation to the pseudo-cubic *P*4/*mmm* structure is observed at such a low temperature as 650 °C.

Lithium Disorder and Mobility Path. The disordered arrangement of Li and La atoms in the unit cell of the RT phase is shown in Figure 4. In space group *I*4/*mcm* ($\sqrt{2}a_p \times \sqrt{2}a_p \times 2a_p$) there is a single independent lanthanum atom per unit cell with about 1/2 statistical occupancy (Table 1), similarly to the $R\bar{3}c$ ($\sqrt{2}a_p \times \sqrt{2}a_p \times 2\sqrt{3}a_p$) structure and

(27) Harada, Y.; Hirakoso, Y.; Kawai, H.; Kuwano, J. *Solid State Ionics* **1999**, *121*, 245.
(28) Bohnke, O.; Duroy, H.; Fourquet, J. L.; Ronchetti, S.; Mazza, D. *Solid State Ionics* **2002**, *149*, 217.

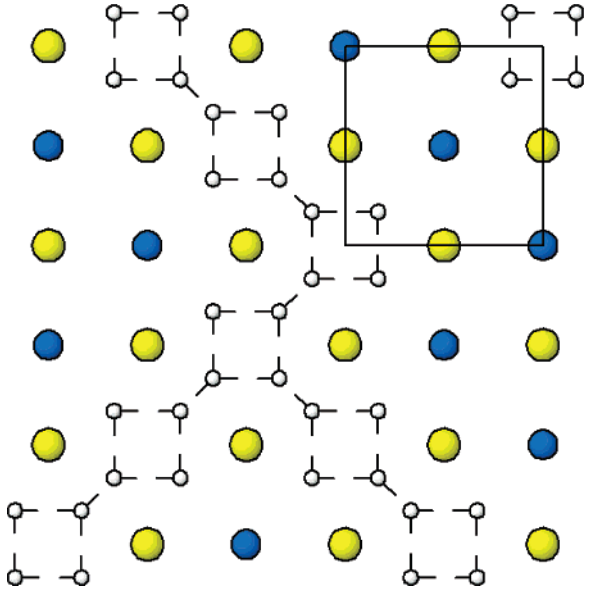

Figure 5. Sketch of the possible two-dimensional diffusion pathway of lithium (small pale spheres) in the (001) planes of quenched $Li_{0.3}La_{0.567}TiO_3$ (*I*4/*mcm* structure). A locally ordered arrangement of La atoms (dark spheres) is shown, taking into account the La−Li avoidance.

at variance with the *Cmmm* ($2a_p \times 2a_p \times 2a_p$) and *P*4/*mmm* ($a_p \times a_p \times 2a_p$) cases,[6,12] where two atoms La1 and La2 with major and minor occupation factors, respectively, are observed. Therefore, no coupled partial ordering of La vacancies and Li interstitials can occur in the average structure of the present case.

Li atoms are not located in the vacant La sites,[6] where they would give rise to unacceptably long Li−O distances (at least 2.60 Å), but in quadruple positions surrounding each La vacancy at a 1.30 Å distance. Every Li position lies at 0.66 Å from the center of the Ti_4O_4 square window perpendicular to the La−La [110] connecting line ("bottleneck" site), and it is firmly bonded to the four O atoms of the window with distances in the range 1.94−2.17 Å and in a very flat pyramidal coordination. Thus, Li is much closer to the bottleneck site than to the La vacancy, but yet it does not lie on it as in other proposed structures of the $Li_xLa_{2/3-x/3}\square_{1/3-2x/3}TiO_3$ family, like the $R\bar{3}c$ and the *Cmmm* ones.[7,13] The shortest contacts between disordered lithium positions are 1.33 (across the bottleneck site) and 1.88 Å long and correspond to incompatible occupation in the same local structure. In particular, out of the quadruplet around a La vacancy only two opposite Li positions (2.60 Å apart) can be occupied together locally.

On looking at Figure 4, the disordered lithium positions appear to be arranged in two-dimensional networks parallel to (001) and separated by *c*/2. The pathway of lithium mobility can then be sketched as a sequence of jumps between adjacent occupied and vacant sites within a single layer. A possible locally ordered pattern of La atoms is shown in Figure 5, which is correlated with a consistent occupation of Li sites avoiding forbidden Li/La short contacts. On the other hand, no ordering scheme appears within the Li pattern, where occupied and empty sites are not distinguished to emphasize the diffusion pathway (dashed lines in Figure 5). A high mobility of Li^+ ions can clearly be predicted on the basis of this structural configuration, because of the quite

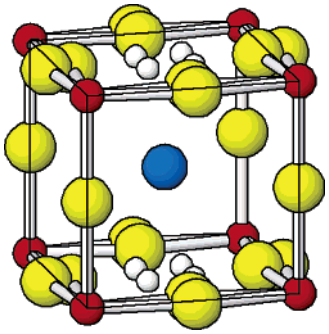

Figure 6. Unit cell content of the *P*4/*mmm* structure of $Li_{0.3}La_{0.567}TiO_3$ at 650 °C, with an origin shift of 1/2, 1/2, 1/2 with respect to the data of Table 2. The lithium atoms are shown as small pale spheres.

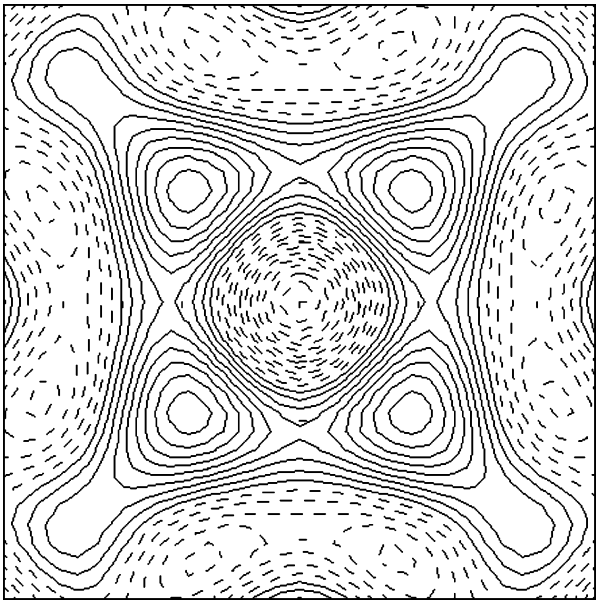

Figure 7. Section at $z = 1/2$ of the Fourier difference map of the *P*4/*mmm* structure of $Li_{0.3}La_{0.567}TiO_3$ at 650 °C (both *x* and *y* in the −1/4 to +1/4 range). Full and dashed contour lines correspond to negative and positive neutron scattering density, respectively. The four negative peaks indicate split positions of the disordered lithium atoms.

short jumping distances of only 1.33 and 1.88 Å. Is the process of ion transport strictly two-dimensionally confined, as implied by the above model? We should remember that a secondary lithium position (Li n.2, cf. Results) was detected in the Fourier map at 1/2, 0, 0.18, that is, vertically below (or above) the La vacancy along the *c* axis. This site, probably characterized by a minor occupancy, is likely to provide the link between mobility networks of adjacent layers spaced by *c*/2. Therefore, the diffusion path is mainly two-dimensional, but connection in the third direction is assured by an additional less populated lithium site.

The unit cell content of the HT phase (*P*4/*mmm* structure) of $Li_{0.3}La_{0.567}TiO_3$ is shown in Figure 6. Lithium is located on the (001) layer of Ti and O1 atoms, instead of that of La and O2 atoms as in the RT phase; its statistical distribution over four equivalent sites is displayed by a Fourier difference map on the layer (Figure 7). The shortest Li−La distance (2.04 Å) is comparable with the sum of the corresponding ionic radii so that both atoms might be present together in the same unit cell. On the other hand, only one of the four disordered sites of Li can be occupied at a time, and, further, the local ordering of Li must be coupled to that of the O1

atoms. A given occupied Li site is consistent with only four out of the eight neighboring O1 positions, achieving a fourfold planar coordination with two short (1.80 Å) and two long (2.20 Å) bonds (Table 2). Taking into account the HT (650 °C), the coupled disorder of Li and O1 atoms is likely to have a dynamic rather than static character. The mechanism of ionic mobility seems to be quite different from that proposed above for the RT structure and probably involves Li jumping into secondary sites located in the La vacancy hollow. Further investigations on the HT behavior of $Li_{0.3}La_{0.567}TiO_3$ are planned in our research.

Conclusions

It has been proved that the liquid-N_2 quenched form of $Li_{0.3}La_{0.567}TiO_3$ shows, at RT, a *I*4/*mcm* superstructure of perovskite with a unit cell of type $\sqrt{2}a_p \times \sqrt{2}a_p \times 2a_p$, corresponding to a thermodynamically metastable phase. This variety of perovskite-derived structure had never been observed before within the $Li_xLa_{2/3-x/3}\square_{1/3-2x/3}TiO_3$ family of lithium ion conductors. An octahedral tilting of type $a^0a^0c^-$ is present, but La shows a single independent site along the *c* axis. The lithium atoms have been found in disordered positions within the cages surrounding lanthanum vacant sites, near the centers of square windows separating adjacent cages. It ensues that ion transport should be based, in this compound, on a two-dimensional mechanism implying a correlated local ordering of La vacancies and occupied Li sites, with ionic hopping between quite close (1.33−1.88 Å) positions. This is consistent with the high lithium mobility observed in this material. At HT a structural transformation occurs, to a *P*4/*mmm* pseudo-cubic configuration where part of the oxygen atoms are disordered and where Li atoms are located in completely different positions with respect to the low-temperature phase. Nonquenched samples of $Li_{0.3}La_{0.567}TiO_3$ are presently under investigation, with the aim of clarifying the role of thermal history on the structural properties of this important ionic transport material.

Acknowledgment. We thank R.M. Ibberson (ISIS Facility, Rutherford Appleton Laboratory, U.K.) for assistance with the neutron diffraction experiment and the Italian C.N.R. for supporting financially the research at ISIS. A PRIN grant from MIUR (Roma) is also acknowledged.

CM060120R